Available online at www.sciencedirect.com
SCIENCE DIRECT®
Journal of Hydrology 296 (2004) 164–178
Journal of Hydrology
www.elsevier.com/locate/jhydrol

Redox zonation at the saline-influenced boundaries of a permeable surficial aquifer: effects of physical forcing on the biogeochemical cycling of iron and manganese

M. Snyder, M. Taillefert*, C. Ruppel

School of Earth and Atmospheric Sciences, Georgia Institute of Technology, 311 Ferst Dr., Atlanta, GA 30332-0340, USA

Received 31 July 2003; revised 3 March 2004; accepted 19 March 2004

Abstract

Research investigating geochemical changes accompanying subsurface mixing of fresh and saline water has primarily focused on cation exchange and mineral dissolution/precipitation reactions. In this study, we report on redox species zonation at the boundaries of a freshwater lens confined beneath a small, permeable island surrounded by saline marshes and tidal creeks and located on the estuary side of Sapelo Island, Georgia. The spatial and temporal distribution of the chemical species in the aquifer implies that the freshwater lens resists saline intrusion by maintaining constant advection across the salinity gradient. As a result, the biogeochemical processes in this aquifer seem to have reached a quasi steady-state very close to equilibrium. Redox reactions associated with natural organic matter oxidation may also play an important role at the salinity transition. Surprisingly, aerobic respiration and microbial iron reduction seem to be the main pathways for natural organic matter oxidation. Sulfate reduction is not significant despite the high concentration of sulfate available, and manganese oxides are probably chemically reduced by dissolved sulfide and Fe^{2+}. This study is the first to demonstrate that iron and manganese reduction takes place at the salinity transitions bounding both sides of an island freshwater lens and that microbial iron reduction accounts for most of anaerobic respiration of natural organic matter at these transitions.

Keywords: Groundwater; Redox; Salinity transition; Iron; Manganese; Sulfide

1. Introduction

Biogeochemical processes involving redox reactions have been extensively studied in freshwater aquifers (e.g. Champ et al., 1979; Von Gunten et al., 1991; Chapelle and Lovley, 1992; Matsunaga et al., 1993; Bourg and Bertin, 1994; Brown et al., 1999; Groffman and Crossey, 1999), but have received less attention in permeable coastal aquifers subject to saline intrusion (Magaritz and Luzier, 1985; Bottrell et al., 1991; Barker et al., 1998; Jakobsen and Postma, 1999; Charette and Sholkovitz, 2002; Testa et al., 2002; Cai et al., 2003). Instead, most investigations in coastal subsurface environments focus on the fate of nutrients (e.g. Valelia et al., 1990; Portnoy et al., 1998; Charette et al., 2001; Tobias et al., 2001a), ion exchange processes (e.g. Appelo and Willemsen,

* Corresponding author. Tel.: +1-404-894-6043; fax: +1-404-894-5638.
E-mail address: mtaillef@eas.gatech.edu (M. Taillefert).

0022-1694/$ - see front matter © 2004 Elsevier B.V. All rights reserved.
doi:10.1016/j.jhydrol.2004.03.019

1987; Moore, 1999), or export of groundwater to marine environments (Valelia et al., 1992; Moore, 1996; Charette et al., 2001; Tobias et al., 2001b).

Saltwater intrusion, which may be driven by a variety of physical processes (Moore, 1999), has a profound effect on freshwater aquifers. Most importantly, saline intrusion is irreversible due to the large concentration gradient between the saline and fresh water endmembers (Chapelle, 1997). The ionic strength changes associated with saline intrusion modify groundwater chemical composition and may dissolve or precipitate carbonate minerals (Valocchi et al., 1981; Appelo et al., 1990; Moore, 1999), with important environmental consequences (Paull et al., 1990). Alternately, the oxidation of natural organic matter in the aquifer may produce excess CO_2 and result in the dissolution of carbonate minerals (Barker et al., 1998; Moore, 1999; Cai et al., 2003). Past efforts to characterize the diagenetic processes associated with the remineralization of natural organic matter have established that sulfate reduction is the main biogeochemical process driving carbon oxidation in brackish aquifers (Magaritz and Luzier, 1985; Barker et al., 1998). Iron reduction may also be significant in such environments (Jakobsen and Postma, 1999) although the relative importance of microbial iron reduction and chemical oxidation of dissolved sulfide is unclear.

During infiltration from an open water reservoir (e.g. a creek) into a permeable surficial aquifer across a creek bank, lateral flow and transport of chemical species largely control the lateral orientation of redox zones. For example, Bourg and Bertin (1994) showed that dissolved oxygen and dissolved organic carbon (DOC) levels dropped sharply in the 10 m closest to the bank, with a subsequent peak in dissolved manganese (Mn_d). Von Gunten et al. (1991) reported similar results in their study of a river-recharged aquifer. Although Jakobsen and Postma (1999) argue for vertical redox zonation (horizontal layering) in their study area, theirs is a particular case in which saline water that originated as sea spray on pine trees infiltrates downward into the aquifer.

Laboratory experiments have been used to develop detailed models for the redox reactions occurring along the infiltration pathway from creek bank to permeable aquifer (Von Gunten and Zobrist, 1993). The resulting redox zones are arrayed from creek bank to aquifer in the order of decreasing free energy yield for microbial reactions associated with natural organic matter oxidation. This study also constrained the kinetics of microbial processes, thereby providing key information about rates of reactions.

Despite these advances, relatively little is known about redox biogeochemical reactions at salinity transitions in coastal surficial aquifers. In this study, we investigate the biogeochemistry of a freshwater aquifer on a small, sand-dominated, permeable island (hammock) completely surrounded by salt marsh and tidal rivers and located on the estuarine side of Sapelo Island, GA, in the backbarrier position. This study is the first to demonstrate that iron and manganese reduction takes place at the salinity transitions bounding both sides of an island freshwater lens and that microbial iron reduction probably accounts for most of anaerobic respiration of natural organic matter at these transitions.

2. Site description

The study site for this research is Moses Hammock, a 0.07 km^2 island of Pleistocene sand and muds lying $\sim$100 m west of the main part of Sapelo Island, GA, one of the major barrier islands within the Georgia Bight (Fig. 1a). During the course of the study, Moses Hammock was designated as a focus site for the National Science Foundation-sponsored Georgia Coastal Ecosystems (GCE) Long Term Ecological Research (LTER) program. Tidally influenced salt marshes of primarily *Juncus Romerianus* and *Spartina alterniflora* border three sides of Moses Hammock, while the eastern side of the site adjoins the Duplin River, which has a tidal range of 2.8 m. The sediments making up Moses Hammock are primarily well-sorted, clean, fine sands with an effective grain size of $\sim$120 μm. Based on laboratory grain size analyses, permeameter tests, aquifer testing, and tidal pumping analyses, Schultz and Ruppel (2002) constrained a range of hydraulic parameters at pore to field scales. Their analyses yield hydraulic conductivity of $\sim 10^{-4}$ to 10^{-5} m s^{-1} for upland sediments, with a creek bank clogging layer having significantly lower hydraulic conductivity.

At the time of this study, a network of $\sim$12 groundwater monitoring wells had been installed on

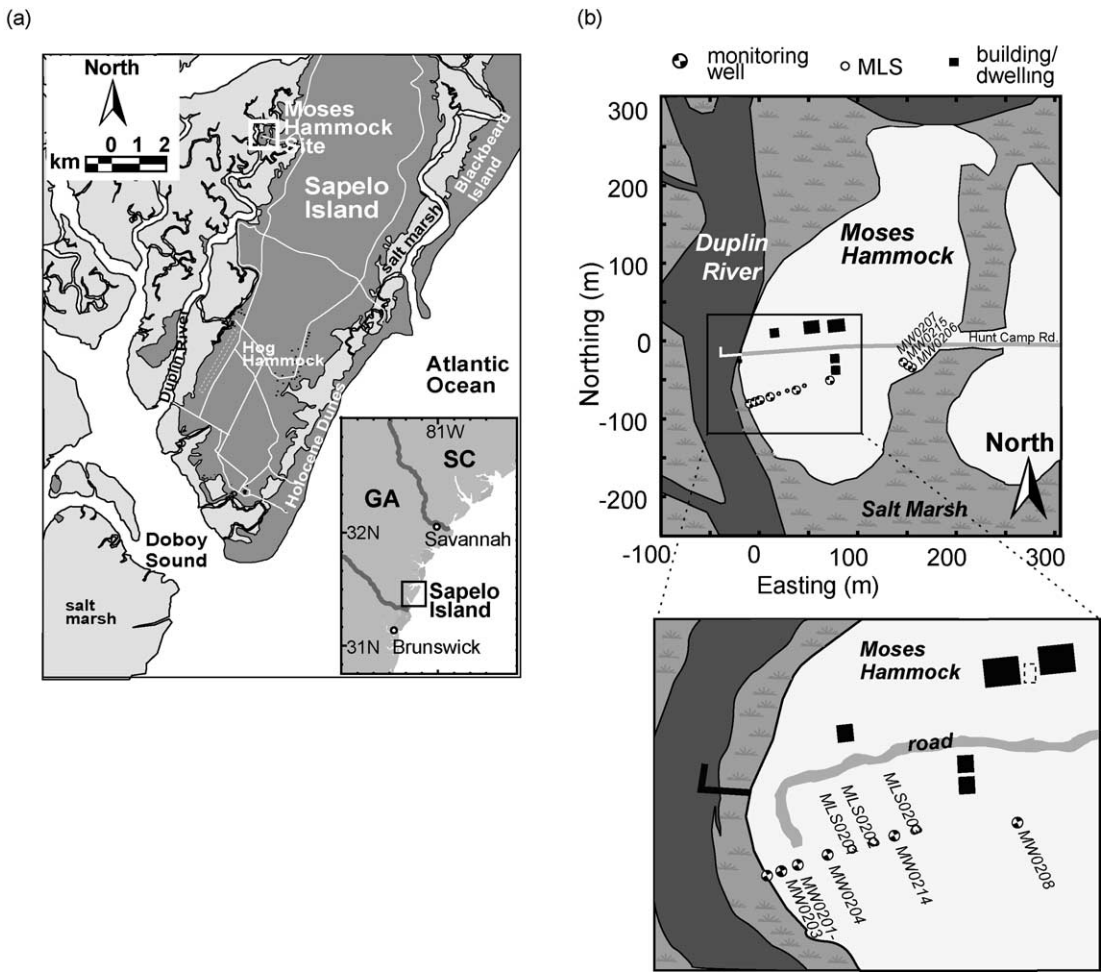

Fig. 1. (a) The regional map shows the location of Sapelo Island, offshore Georgia in the South Atlantic Bight. The location of Moses Hammock relative to major tidal tributaries, the main part of Sapelo Island, and the salt marsh complex is shown on the larger digital elevation map. (b) This map shows only the location of the wells referred to in this study. At the time of this study, Moses Hammock had 12 monitoring wells along the transect (Schultz, 2002), and three MLS were installed during this study. The wells are oriented along a transect roughly perpendicular to the river bank, stretching ~170 m between the Duplin River on the west and the salt marsh on the east. Well parameters are given in Tables 1 and 2.

Moses Hammock (Schultz and Ruppel, 2002) along a ~180 m transect between the Duplin River on the west and the salt marsh on the east (Fig. 1b). These wells and a coincident set of three multilevel sampling wells (MLS) installed late in this study (Snyder, 2002) provided constraints on both the lateral and vertical distribution of chemical species in the aquifer (Fig. 1b). Tables 1 and 2 give the characteristics of the wells used in this study. Standard monitoring wells were installed through a hand-augered borehole, and a coarse sand filter pack was emplaced around the screened intervals before backfilling of the hole with native sediment. The wells were finished with a concrete surface seal to prevent annular flow and a locking metal or plastic cap to provide wellhead security. Monitoring wells consist of 3.2 or 5.1 cm ID Schedule 40 PVC risers with high flow 0.15 mm machine-slotted screens forming the deepest part of the well above the well point. All wells are partially penetrating, with screens deep enough to be below the water table at all times. MLS were constructed using a technique modified from Stites and Chambers (1991) and were installed through a steel pipe drive assembly that was then removed to leave the sampling ports in

Table 1
Characteristics of monitoring wells (MW) and multi-level sampling wells (MLS) at Moses Hammock

Sampling sites	Distance from Duplin River (m)	Sampling depth (m)
Duplin river	0	0
MW0201	4.2	−3.82
MW0202	8	−4.14
MW0203	14	−4.06
MW0204	26	−4.54
MLS0201	33.4	Table 2
MLS0202	39.6	Table 2
MW0214	45.9	−4.39
MLS0203	52.4	Table 2
MW0208	89.3	−4.38
MW0206	151.8	−4.15
MW0215	160	−4.12
MW0207	162	−3.49
Saltmarsh	171	0

Sampling depth refers to the middle of the screened interval for monitoring wells.

direct contact with the sediments. More details about the MLS are given by Snyder (2002).

Except for sporadic pumping from the deep confined Floridan aquifer to supply the needs of a hunt camp, precipitation is the only source of freshwater and recharge for the hammock's surficial aquifer. As predicted by modified Dupuit–Ghyben–Herzberg theory (Urish, 1980), geophysical imaging and direct sampling in monitoring wells reveal the presence of a freshwater lens whose center lies just eastward of the middle of the hammock (Schultz, 2002). The morphology of the lens is asymmetric, with its thickest part skewed toward the east (marsh) side, consistent with higher mean water level on the Duplin River side of the hammock. Although many factors including precipitation, semi-diurnal tidal cycles, and sediment heterogeneity influence the magnitude and direction of groundwater flow, freshwater flow in the lens is generally from its center toward the edges of the aquifer (Schultz, pers. comm. 2000).

Table 2
Characteristics of multiple level sampling (MLS) wells

MLS wells	Port	Sampling depth (m)
MLS0201	(1)	−2.31
	(2)	−2.93
	(3)	−3.55
	(4)	−4.17
MLS0202	(1)	−2.31
	(2)	−2.93
	(3)	−3.22
	(4)	−3.84
MLS0203	(1)	−1.59
	(2)	−2.21
	(3)	−2.83
	(4)	−3.45
	(5)	−4.07

Geophysical and hydrologic investigations conducted on Moses Hammock since 1998 had constrained the distribution of fresh and saline water in the subsurface prior to the initiation of the geochemical research (Schultz, 2002). Direct measurement of groundwater conductivity in monitoring wells and constraints from geophysical (inductive electromagnetic and DC resistivity) surveys indicated the presence of high salinity groundwater to a distance of ~28 m into the upland adjacent to the Duplin River on the western side (close to MW0204) and ~20 m adjacent to the periodically flooded salt marsh on the eastern side. The absolute extent of the lateral intrusion of saline water is relatively constant over interannual cycles, but drought episodes and changes in the salinity of the tidal creek have an impact on the volume of freshwater in the lens and the salinity of intruded water, respectively, as shown by Schultz (2002). Bank morphology appears to radically affect the dynamics of saline intrusion into the surficial aquifer and the physical forcing of the aquifer by tidal fluctuations both at this site and other Sapelo Island sites (Schultz, 2002; Schultz and Ruppel, 2002).

3. Methods

3.1. Water sampling and measurements

Groundwater and surface water samples for this study were collected 11 times between June 2000 and May 2001. For the conventional groundwater wells, we sampled from the deepest parts adjacent to the screens using hard polyethylene tubing connected to a peristaltic pump. To ensure representative sampling of aquifer water, wells were first purged of one to two well volumes at a high rate. For MLS wells, which yield only low volume samples, we purged briefly at

low rates before collecting the groundwater samples. During sampling, water was pumped into a polycarbonate flow cell to prevent contact with the atmosphere, with pumping continuing until electrodes measuring pH, dissolved oxygen (YSI-55), and conductivity, salinity, and temperature (WTW CST combination) reached equilibrium. The salinity measurements were used to calibrate the dissolved oxygen (DO) meter. The potential was recorded and converted to pH with the Nernst equation using the in situ temperature (Skoog and Leary, 1996). Reference solutions were conventional buffers (Fisher Scientifics) for low ionic strength waters and TRIS buffers in 0.54 M NaCl (Dickson, 1993) for saline waters.

To prevent oxygen contamination, water samples were collected in acid-washed 60 ml polypropylene syringes with teflon plungers (HSW) fitted directly to the sampling tubing. Once filled, syringes were placed in a plastic bag continuously overfilled with N_2 gas. The samples were stored in the dark and at 4 °C until analysis or preservation within 6 h.

3.2. Laboratory analyses

Alkalinity was determined as total alkalinity in unacidified samples by potentiometric titration with a 0.5 M HCl stock solution. The titrant was prepared at three ionic strengths (0.7, 0.35, and 0 M NaCl) to account for the salinity changes in the aquifer. A combination microelectrode (Corning) was used with an Orion pH meter, and the equivalence points were determined with the Gran (1952) method.

Iron and sulfide were analyzed colorimetrically with a Milton Roy UV/Vis Spectrophotometer within 3 h of sampling. Samples were filtered through 0.45 μm membrane Acrodisc syringe filters (Whatman). Total dissolved iron (Fe_d) and dissolved Fe^{2+} were determined using the ferrozine method with and without hydroxylamine hydrochloride, respectively (Stookey, 1970). Dissolved ferric iron ($Fe^{(III)}_{(aq)}$) was obtained by subtracting Fe^{2+} from Fe_d. Dissolved sulfide ($\sum H_2S = H_2S + HS^- + S^{2-}$) was measured using the Cline (1969) method. Filtered samples were also preserved unacidified for chloride, nitrate, and sulfate analysis.

Chloride, nitrate, and sulfate concentrations were determined by ion chromatography using a Dionex DX-300 series analyzer with a conductivity detector. Samples were eluted through an AG4 guard column and an AS4 analytical column (Dionex) with a 3.6 mM $NaHCO_3$/3.8 mM $NaCO_3$ buffer solution. A 25 mM H_2SO_4 solution was used as regenerant. For these measurements, high salinity samples were diluted between 50 and 100 times with deionized water. Dissolved manganese (Mn_d) was analyzed with a graphite furnace atomic absorption spectrophotometer (GFAAS) with Zeeman correction (Varian 600).

Samples were collected for DOC analysis in glass syringes, filtered on 0.7 μm GFF filters (Whatman), and stored in dark glass bottles at 4 °C until analysis within a few days. DOC was determined by the combustion method with a Shimadzu TOC-5050A analyzer equipped with an autosampler. Just before analysis, the samples were acidified to pH <2 with a 2N HCl solution and purged with UHP grade helium to remove dissolved inorganic carbon. The instrument was calibrated with potassium hydrogen phthalate standards.

4. Results

4.1. Wellside geochemistry

A basic suite of water parameters, including conductivity, temperature, dissolved oxygen, and pH, were repeatedly measured between July 2000 and May 2001 to constrain temporal changes in groundwater and surface water properties. Unless stated otherwise, the standard deviations represent the temporal variations in these wells. As demonstrated in Fig. 2, Moses Hammock is characterized by two high salinity zones (average conductivity of ~ 38 mS cm^{-1}) that confine the surficial freshwater aquifer (conductivity below detection limit) to the middle of the hammock. The geochemical results indicate that the lateral extent of the saline intrusion is greater (>46 m) on the Duplin River side of the hammock than on the salt marsh side (~ 20 m), consistent with numerous geophysical surveys and conductivity measurements of groundwater dating back as far as 1998 (Schultz and Ruppel, 2000; Schultz, 2002). The groundwater displayed little variation (± 3.4 mS cm^{-1}) in conductivity over the 11 months of this study, which confirms geophysical

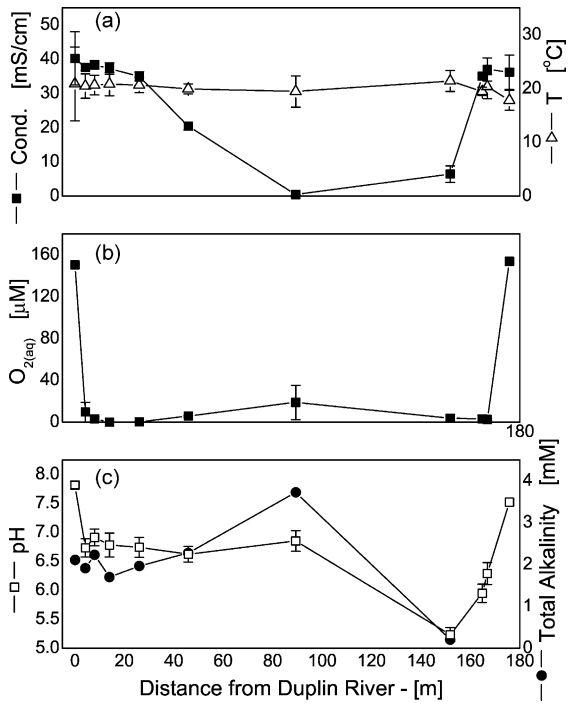

Fig. 2. Average values of various parameters for surface water from Duplin River (left side) and salt marsh (right side) and groundwater in monitoring wells at Moses Hammock. Panels show average (a) conductivity and temperature, (b) dissolved oxygen and (c) pH and total alkalinity for nine sampling trips between June 2000 and May 2001 as a function of distance from the Duplin River. Except for total alkalinity, which was measured only in March 2001, the standard deviations shown here represent the temporal variation of each parameter.

results that imply that the saline intrusion and lens morphology have reached a steady-state (Schultz, 2002).

In general, groundwater temperatures were relatively constant over the course of the study (Fig. 2a). The Duplin River displayed the largest temperature variation (±7 °C) while the salt marsh had the lowest temperature (mean 17.8 °C) of any water sampled over this period. The freshwater endmember (MW0208) had the lowest average groundwater temperature (19 °C) and the largest temporal variation (±3 °C) over the course of the study.

Except in the freshwater wells (MW0208), where the DO concentration reached 19 μM, groundwater values were typically below the detection limit and at ~65–70% of saturation in the Duplin river and the salt marsh (Fig. 2b). Interestingly, the largest temporal variation (±16 μM) in DO over the sampling period was found in the freshwater endmember. Low DO content and low temporal variability of dissolved oxygen indicate that the groundwater has reached a suboxic state in which the supply of oxygen is partially balanced by aerobic respiration of natural organic matter or oxidation of reduced chemical species (i.e. Fe^{2+}, Mn^{2+}, $\sum H_2S$).

The average Duplin River pH was 7.8, while the average pH of salt marsh waters was 7.5 (Fig. 2c). Groundwater pH was almost one pH unit lower than that of the adjacent Duplin River or salt marsh, varying between 5.2 (MW0206) and 6.9 (MW0202). In addition, the pH gradient from the salt marsh to the hammock's freshwater interior was much stronger than that from the Duplin River to the same freshwater well (MW0208), following the same pattern as conductivity and other measurements.

4.2. Total alkalinity and dissolved organic carbon

Total alkalinity was measured to determine the extent of natural organic matter mineralization during one sampling trip (March 2001). Total alkalinity varied between ~2 mM in the Duplin river and the saline aquifer on the side of the Duplin river to a maximum of 4 mM in the freshwater endmember (Fig. 2c). It then decreased to a minimum of 300 μM within 150 m from the Duplin river. No data were collected on the salt marsh side.

DOC was measured only once in October 2001 (S. Sibley, pers. comm., 2001; Fig. 3a). DOC varied between 4 and 6 mgC l^{-1} in the saline side near the Duplin River, increased to 13 mgC l^{-1} within 25 m from the Duplin river, before decreasing to a minimum value of 3 mgC l^{-1} at 150 m from the Duplin river. Interestingly, the minimum DOC coincided with the lowest total alkalinity and pH detected in the aquifer. Finally, DOC rose again to a maximum concentration of 12.5 mgC l^{-1} near the salt marsh.

4.3. Redox chemical species

Dissolved manganese, dissolved ferrous and ferric iron, sulfate, and dissolved sulfide were measured between June 2000 and May 2001. The concentration of dissolved manganese (Mn_d) was generally low but

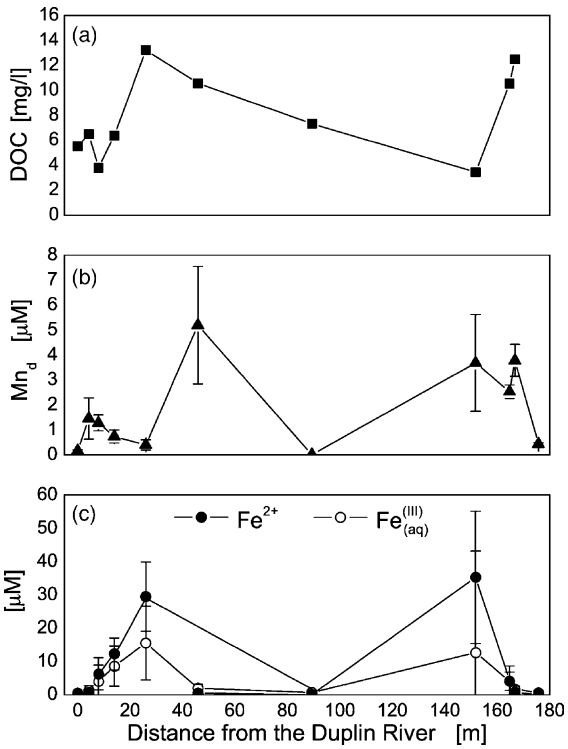

Fig. 3. Average concentrations of (a) dissolved organic carbon (DOC); (b) dissolved manganese; and (c) Fe^{2+} and $Fe^{(III)}_{(aq)}$ for samples obtained between June 2000 and May 2001 as a function of distance from the Duplin river. Except for DOC, which was measured only in October 2001 (S. Sibley, pers. comm., 2001), the standard deviation represents the temporal change in each species.

displayed three distinct maxima along the hammock groundwater transect. Mn_d increased from submicromolar values in the Duplin river to reach a first maximum of 1.5 μM just inside the aquifer at the edge of the upland (MW0201). With greater distance from the upland edge, Mn_d decreased within the high salinity wedge to submicromolar levels within 25 m from the Duplin river (MW0204). Still within the salinity gradient, Mn_d reached a second maximum of 5.2 μM at ~45 m from the Duplin river (MW0214) and subsequently decreased to near detection limit concentrations in the freshwater endmember (MW0208). A third maximum of 3.7 μM occurred ~150 m from the Duplin River in MW0206, within 25 m of the edge of the salt marsh bounding the east side of the hammock, and remained at about this level before decreasing to submicromolar levels in the salt marsh. Temporal fluctuations in Mn_d were generally significant, ranging from 3 nM to 2.4 μM or up to 53% relative change in some wells.

Dissolved ferrous iron (Fe^{2+}) reached much higher concentrations in groundwater than Mn_d and displayed two distinct peaks along the groundwater transect (Fig. 3c). Fe^{2+} concentration was below detection limit in both the Duplin River and the salt marsh. With increasing distance from the upland edge at the Duplin River, Fe^{2+} increased to reach a maximum of 29.5 μM at ~25 m from the upland edge (MW0204) before decreasing to submicromolar levels in the freshwater endmember (MW0208). Proximal to the salt marsh on the east side of the island, Fe^{2+} reached a second maximum of 35 μM within the salinity gradient. This spatial pattern was persistent over the duration of this study with the most important temporal variations in the wells with the highest concentrations of Fe^{2+}. Interestingly, dissolved ferric iron ($Fe^{(III)}_{(aq)}$) concentrations matched the pattern of spatial and temporal variations in Fe^{2+} but with higher amplitudes in the wells with the highest concentrations of $Fe^{(III)}_{(aq)}$. $Fe^{(III)}_{(aq)}$ peaked at 15.5 μM at MW0204 on the Duplin river side and at 12.6 μM in MW0206.

To determine the significance of sulfate reduction, sulfate (SO_4^{2-}) and dissolved sulfide ($\sum H_2S$) were measured over most of the study period (Fig. 4).

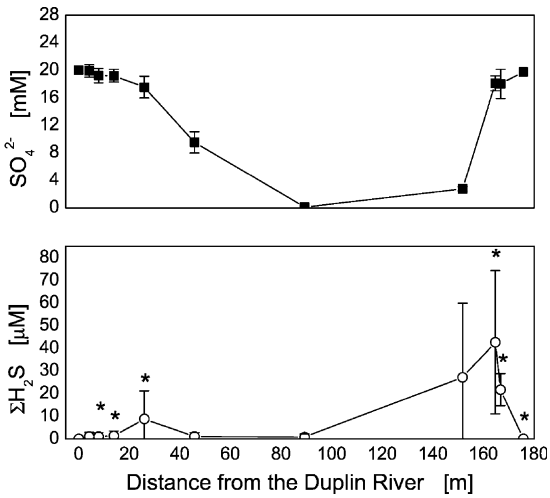

Fig. 4. Average sulfate and dissolved sulfide ($\sum H_2S$) in Moses Hammock from November to May 2001 as a function of distance from the Duplin river. The standard deviation represents the temporal variation in each well. The stars indicate the wells in which FeS precipitation is predicted at equilibrium.

In both the Duplin River and the salt marsh, SO_4^{2-} concentrations were ~20 mM or 70% of standard seawater. The average concentration decreased slightly to ~17.5 and 18 mM in the high salinity zones near the Duplin river and the salt marsh, respectively, and was negligible in the freshwater endmember (MW0208). Dissolved sulfide was generally present in groundwater only at low concentrations during the duration of this study and was below detection limits in both the Duplin River and the salt marsh. On the Duplin River side of the hammock, $\sum H_2S$ remained close to the detection limit in the part of the aquifer close to the creek bank, peaking at 9 μM at the salinity transition (26 m from the Duplin River) before decreasing to close to the detection limit in the freshwater endmember (MW0208). Continuing across the hammock toward the salt marsh, $\sum H_2S$ concentration increased to a maximum of ~42 μM at MW0206, 11 m from the salt marsh. The temporal variation of dissolved sulfide was the greatest of any species we measured, as reflected by the standard deviations in Fig. 4. In contrast, the concentration of sulfate varied only slightly (4–11% relative change).

4.4. Depth profiles of chloride and sulfate at the salinity transition

To provide additional constraints on the concentration of chemical species in the aquifer, we sampled groundwater at discrete depths in three MLS wells along the monitoring wells transect (Fig. 1b). Fig. 5 shows a composite of the chloride and sulfate results acquired in the MLS wells for the May 2001 sampling trip as a function of both depth below ground surface and distance from the Duplin River. For reference, the average concentrations of the monitoring wells closest to these MLS wells are also provided in Fig. 5. Chloride and sulfate concentrations increase linearly as a function of depth in MLS0201, and the concentration in the deepest port is consistent with Cl^- and SO_4^{2-} concentrations in the nearby MW0204 well. Groundwaters from MLS0202, which is more proximal to the freshwater part of the lens aquifer, show a concave upward pattern in both Cl^- and SO_4^{2-}, and the lowermost port clearly samples the transition zone that separates the fresher, less dense water from the underlying saline water collected in the nearby

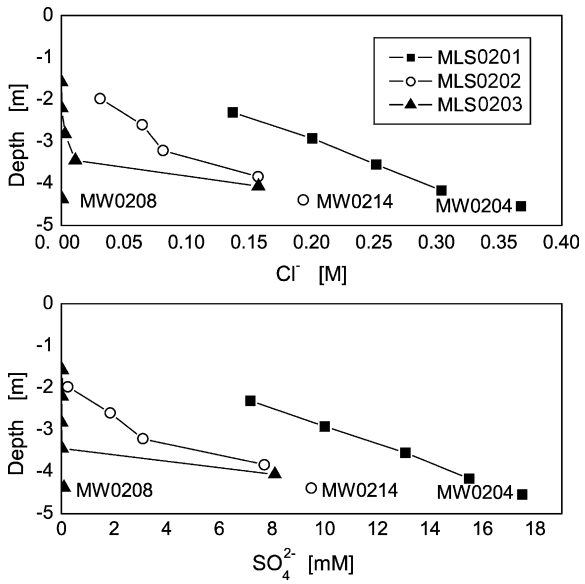

Fig. 5. Depth profiles of: (a) chloride and (b) sulfate concentrations in MLS0201, MLS0202, and MLS0203 in May, 2001. The average concentrations of chloride and sulfate found in the monitoring wells closest to these MLS wells are provided for reference. MLS0201 is 7 m east of MW0204, MLS0202 is 8 m west of MW0214, and MLS0203 is 8.5 m east of MW0214 and 39 m west of MW0208.

MW0214. Finally, Cl^- and SO_4^{2-} concentrations are below detection limits at depths shallower than 3.5 m in MLS0203, but the deepest port samples the same transition zone water as MW0214 and the deepest port at MLS0202.

5. Discussion

5.1. Stability of the freshwater lens and redox zonation

All of the geochemical parameters are consistent with the presence of a well-developed freshwater lens beneath the center of Moses Hammock, which serves as an apt microcosm for a large, permeable barrier island. Along the monitoring well transect, saline water intrudes from both sides—the Duplin River on the west and the salt marsh on the east. This 11-month investigation demonstrates that the two salinity transitions bordering the freshwater aquifer are stable, with very little change in the absolute extent of lateral saline intrusion in the aquifer. These data suggest that

lateral advection away from the center of the freshwater lens toward both the river and the salt marsh balances chemical diffusion of ions from the saline portions of the groundwater towards the aquifer's interior. This advective transport must be in an approximate steady-state to produce such a stable distribution of chemical species within the groundwater over the course of this study. A preliminary investigation conducted by Snyder (2001) also demonstrates that tidal exchange at the edges of this aquifer at the locations sampled by the upland monitoring wells is at the limit of detection. Thus, either the wells do not intersect the part of the saline wedge that experiences rapid exchange or temporal variations associated with advective or diffusive processes occur over time scales greater than a day.

Precipitation during the duration of the groundwater geochemistry study was 58% of the average calculated for the comparable part of the annual cycle for 35 years for which complete data were available between 1957 and 2001. The study period followed years in which precipitation was 67% (1998–1999) and 93% (1999–2000) of the average value. Reduced precipitation leads to less recharge of the freshwater lens and thus smaller hydraulic gradients and less advective transport from the center of the island to the edges. During periods of greater recharge, advection from the center of the lens may outpace diffusion of salt from the saline wedge into the edge of the freshwater lens, resulting in net freshening of the saline wedge. As noted above though, the absolute lateral extent of the saline intrusion appears to be static regardless of seasonal to interannual changes in recharge. Thus, recharge-driven changes in the balance between diffusion and advection apparently affect the salinity of the saline wedge and the width of the mixing zone between the freshwater lens and saline wedge, perhaps without affecting the extent of the intrusion.

The biogeochemistry of the aquifer is strongly influenced by physical forcing associated with the balance between advective outflow from the center of the freshwater lens and opposing diffusion of ions inward from the saline groundwater wedges. The existence of a permanent salinity gradient maintained by advection of freshwater promotes redox zonation that appears to have reached an approximate steady-state. Dissolved oxygen is consumed across the salinity transition either by respiration of natural organic matter or oxidation of reduced chemical species (i.e. Fe^{2+}, Mn^{2+}, and $\sum H_2S$). In contrast, the average concentration of DO and the degree of temporal variation are slightly larger in the middle of the freshwater aquifer, suggesting periodic recharge of the freshwater lens by precipitation.

Metal reduction appears to dominate redox reactions in the saline groundwater wedges. Sulfate reduction occurs on both saline sides of the freshwater aquifer but is less significant than would normally be expected in waters with such high concentrations of sulfate. The average sulfate concentration is closely correlated with the average chloride concentration in most wells (Fig. 6), indicative of conservative seawater dilution behavior. Only wells that sample groundwater within the salinity transitions on both sides of the freshwater lens reveal slightly non-conservative behavior for sulfate, and these wells also contain dissolved sulfide. The same characteristics are found with depth in this aquifer. Between 35 and 55 m distance from the Duplin River, the sulfate and chloride concentrations are closely correlated as a function of depth (Fig. 7), which suggests that little sulfate reduction occurs at shallow depth in the aquifer. Owing to the high background concentration of sulfate in this seawater-influenced aquifer, it is difficult to assess sulfate reduction from sulfate

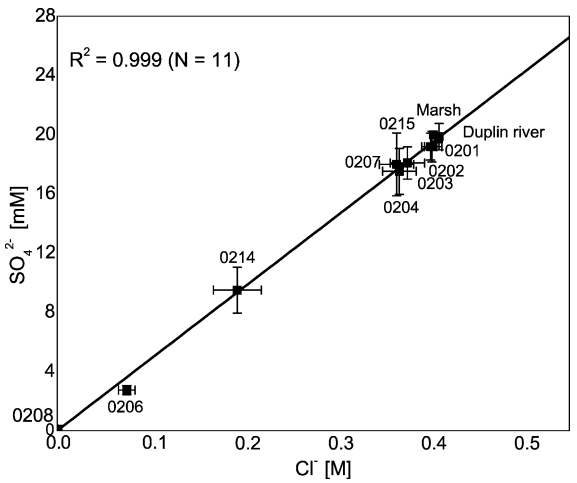

Fig. 6. Correlation between average sulfate and chloride concentrations in the monitoring wells of Moses Hammock aquifer from January 2001 to May 2001.

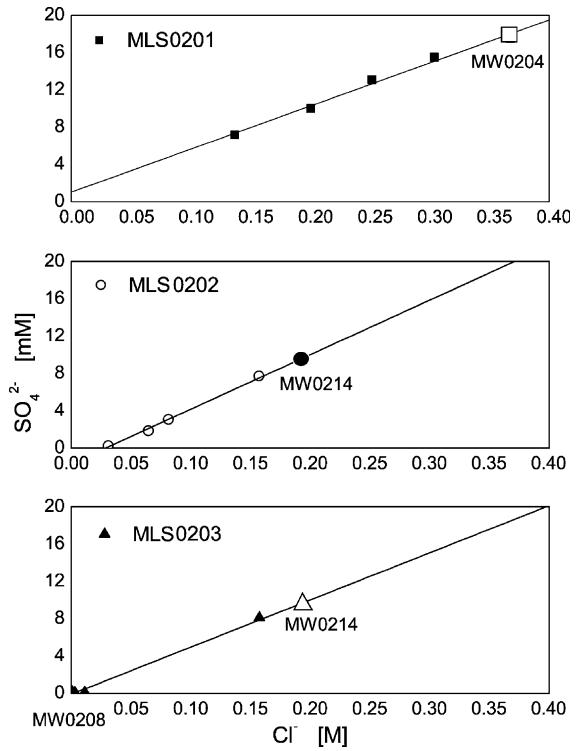

Fig. 7. Correlation between chloride and sulfate concentrations in the different multi-level sampling wells (MLS) in May 2001.

measurements alone. It should also be noted that dissolved sulfide may not accurately reflect sulfate reduction: Dissolved sulfide may reduce iron and manganese oxides (Pyzik and Sommer, 1981; Yao and Millero, 1996), and Fe^{2+} present in the aquifer may remove excess $\sum H_2S$ through formation of iron sulfur minerals (Pyzik and Sommer, 1981).

5.2. Precipitation of iron sulfide minerals

Since the chemical characteristics of the groundwater are nearly at steady-state, the biogeochemical reactions can be considered at equilibrium, and a thermodynamic model can be applied to determine if iron sulfur minerals are oversaturated in this system. We used PHREEQCI (Parkhurst, 1995) to calculate the chemical speciation in the dissolved phase for each well and for the surface water endmembers (salt marsh and Duplin River). Input parameters were temperature, pH, Na^+, K^+, Mg^{2+}, Ca^{2+}, Cl^-, SO_4^{2-}, $\sum H_2S$, Fe^{2+}, and Mn^{2+}. The measured total alkalinity was used to define the carbonate system. The electron activity was fixed by the S(VI)/S(-II) redox couple in anoxic wells containing dissolved sulfide and by the Fe(III)/Fe(II) system in anoxic wells lacking dissolved sulfide. The program calculated charge balance, ionic strength, activity of each species, component speciation among dissolved complexes, and the saturation index of the samples with respect to mineral phases. In all the wells, the calculation predicted a slight excess in positive charges, suggesting that some anions were not considered in the model. However, the excess positive charge was always smaller than 10%, meaning that the charge imbalance should not significantly affect the results.

The thermodynamic results, which are summarized in Table 3, show that sulfide minerals (i.e. $FeS_{(ppt)}$, mackinewite, pyrite, and elemental sulfur) are above saturation in the wells containing dissolved sulfide only (highlighted by stars in Fig. 4b). This outcome suggests that iron sulfide precipitation is only a significant process in the saline portion of the aquifer. The model results given in Table 3 also reveal that other mineral phases are undersaturated or close to saturation in the aquifer, suggesting that the system may be at equilibrium. We therefore conclude that sulfate reduction is only significant in the high salinity wells.

The fact that sulfate reduction is not significant in the freshwater zone indicates that mineralization of natural organic matter in the center of the aquifer is probably achieved primarily with oxygen, manganese oxides, and iron oxides as terminal electron acceptors. Since neither Fe^{2+} nor Mn^{2+} is produced in appreciable quantities, it is reasonable to conclude that aerobic respiration is the dominant pathway for carbon remineralization in the freshwater part of the aquifer.

5.3. Biogeochemical processes: microbial and chemical reduction of manganese and iron oxides in the aquifer

The most important biogeochemical processes within this permeable surficial aquifer occur within the salinity transitions. Fig. 8 summarizes the transport processes, redox reactions, and hydrologic and biogeochemical processes occurring in this system. The formation of several peaks of dissolved

Table 3
Saturation indices of relevant mineral phases calculated by PHREEQC

Sample	Saturation indices							
	Gypsum	Calcite	Dolomite	Aragonite	$FeS_{(ppt)}$	Mackinawite	Pyrite	Sulfur
Duplin	−0.76	0.22	1.33	0.07	n.a.	n.a.	n.a.	n.a.
MW0201	−0.82	−0.84	−0.8	−0.99	n.a.	n.a.	n.a.	−3.22
MW0202	−0.8	−0.58	−0.39	−0.73	−1.37	−0.63	7.95	−3.41
MW0203	−0.79	−0.79	−0.8	−0.93	−0.87	−0.13	8.67	−3.19
MW0204	−0.8	−0.75	−0.76	−0.9	0.49	1.22	10.81	−2.38
MW0214	−0.9	−0.77	−0.99	−0.92	n.a.	n.a.	n.a.	−5.6
MW0208	−2.42	−0.24	−1.55	−0.39	n.a.	n.a.	n.a.	n.a.
MW0206	−1.69	−3.64	−6.42	−3.79	−1.7	−0.97	9.85	−1.14
MW0215	−0.78	n.a.	n.a.	n.a.	−0.74	−0.01	22.71	10.73
MW0207	−0.77	n.a.	n.a.	n.a.	−0.61	0.12	10.78	−0.83
Saltmarsh	n.d.	n.d.	n.d.	n.d.	n.d.	n.d.	n.d.	n.d.

Data used were average concentrations over the year long study. n.a., not applicable; n.d., not determined.

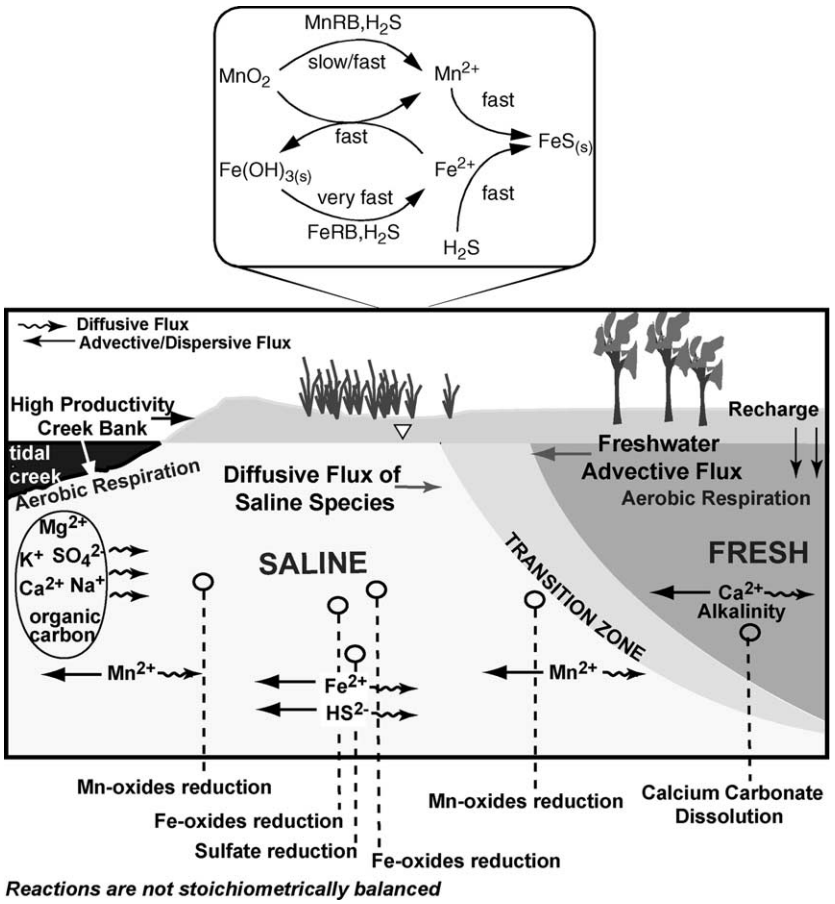

Fig. 8. Schematic diagram representing transport processes and the biogeochemical cycles of manganese, iron, and sulfur across the Moses Hammock aquifer. MnRB, manganese reducing bacteria; FeRB, iron reducing bacteria.

Mn (Mn_d) and Fe^{2+} may be explained by a combination of chemical and microbial metal reduction, mineral precipitation, and adsorption. The first peak of Mn_d within 10 m of the Duplin river most likely reflects chemical reduction of manganese oxide by Fe^{2+} (Postma, 1985; Myers and Nealson, 1988)

$$MnO_{2(s)} + 2Fe^{2+} + 4H_2O \rightarrow Mn^{2+} + 2Fe(OH)_{3(s)} + 2H^+ \quad (1)$$

and/or dissolved sulfide (Yao and Millero, 1996)

$$MnO_{2(s)} + H_2S + 2H^+ \rightarrow Mn^{2+} + S^0 + 2H_2O \quad (2)$$

because the concentration of Fe^{2+} (Fig. 3c) and dissolved sulfide (Fig. 4) are both low at this location. These species could still be provided by diffusion from the interior of the aquifer (i.e. within 28 m from the Duplin river) and could explain the high temporal variations measured in the wells with high concentrations of Fe^{2+} and dissolved sulfide.

The relatively low concentration of DOC within 20 m of the Duplin River (Fig. 3a) is also consistent with lower rates of mineralization of natural organic matter. Interestingly, the reduction rate of manganese oxides by dissolved sulfide (Burdige and Nealson, 1985; Yao and Millero, 1996) is much slower than that by Fe^{2+} (Postma, 1985), strongly suggesting that Fe^{2+} may be the major reductant of manganese oxides at this location. The observed change in pH, which decreases from the edge of the upland near the Duplin River toward the interior of the aquifer, corroborates this interpretation.

It is difficult to attribute the second peak (~45 m from the Duplin River) of Mn_d to chemical reduction of manganese oxides with $\sum H_2S$ since there is little sulfate reduction in this region of the aquifer. Although the microbial reduction of manganese oxides might offer one explanation for this Mn_d peak given the relatively high DOC at this location (Fig. 3a), such a process would produce much more Mn_d than we measured. In turn, this second peak might also be attributed to chemical reduction of manganese oxides by Fe^{2+} diffusing 28 m from the Duplin river. Alternately, Mn_d could be produced significantly by microbial or chemical reduction in the saline region near the Duplin river and removed by adsorption onto sulfide minerals (Arakaki and Morse, 1993) or other solid phases (e.g. Nyffeler et al., 1984), producing a deflection in the Mn_d concentration at 28 m from the Duplin river. As Mn^{2+} is very easily removed by adsorption onto mineral surfaces, this eventuality cannot be neglected. Inversely correlated with the two Mn_d peaks is the peak in Fe^{2+} concentration at 28 m from the Duplin River. The relatively high DOC at this location may be consistent with microbial reduction of iron, but chemical reduction by dissolved sulfide might also occur in this region of maximum $\sum H_2S$ production.

$$2Fe(OH)_{3(s)} + H_2S + 4H^+ \rightarrow 2Fe^{2+} + S^0 + 6H_2O \quad (3)$$

One problem with this interpretation is that the concentration of dissolved sulfide in this region of the aquifer is only about half that required to chemically produce 30 μM of Fe^{2+}, while the concentration of Mn^{2+} required to produce the remaining Fe^{2+} would be the double of the highest Mn_d concentration detected in this aquifer. The fact that Fe^{2+} persists in a location at which iron sulfur minerals precipitate indicates that iron reduction is probably primarily microbially mediated in this region of the aquifer.

Peaks in Mn_d and Fe^{2+} concentrations in the aquifer adjacent to the salt marsh side of the hammock can be explained in similar ways. The two Mn_d peaks probably result from reduction of manganese oxide by Fe^{2+} and dissolved sulfide. This explanation is supported by the rapid rate of Fe^{2+} oxidation by manganese oxides, the fact that there is enough dissolved sulfide generated by sulfate reduction on the saltmarsh side of the aquifer, and that the concentration of Mn_d is too low to be the result of microbial manganese reduction. The strong peak in Fe^{2+} concentration produced at ~150 m from the Duplin River can most likely be attributed to microbial iron reduction since Fe^{2+} can only coexist with dissolved sulfide in excess of the solubility product of FeS if it is produced faster than FeS. Interestingly, the pH at this location is the lowest recorded in the aquifer. Since both microbial and chemical iron reduction by dissolved sulfide consume protons, the low pH can only be the result of FeS precipitation.

Chemical gradients in Fe^{2+}, Mn^{2+}, $\sum H_2S$, and DOC at the salinity transitions of the freshwater lens in Moses Hammock indicate that the aquifer is dominated by microbial iron reduction at the saline

boundaries. Sulfate reduction occurs simultaneously but to a significantly smaller extent. As a result, both microbial processes generate enough reductants that diffuse laterally to reduced manganese oxides. Microbial manganese reduction is possible in this system, but previous studies have shown that reduction of manganese oxides is accelerated by chemical reactions with dissolved sulfide produced by sulfate reducing bacteria (Burdige and Nealson, 1985), especially at pH <7 (Yao and Millero, 1996). The low Mn_d concentrations imply that manganese reduction is either chemical only or balanced by extensive adsorption of Mn^{2+} onto solid phases.

These data corroborate the findings of Jakobsen and Postma (1999), who determined that sulfate reduction is slow and kinetically controlled by fermentation in a freshwater aquifer subject to saline intrusions, while microbial iron reduction depends largely on the reactivity of iron oxides. Although the concentrations of iron, sulfur, and DOC in the aquifer are anticorrelated with those of the sandy aquifer studied by Jakobson and Postma, both studies suggest that metal reducing bacteria can outcompete sulfate reducing bacteria in the subsurface, even at high sulfate concentrations. Recharge of the freshwater aquifer in the middle of the hammock may add enough oxygen to keep the groundwater in suboxic conditions and maintain a dynamic cycle between Fe^{2+} and iron oxides at the saline boundaries.

6. Conclusions

The biogeochemical processes involving iron, manganese, and sulfur at the salinity transitions bounding both sides of a freshwater lens within a small, permeable hammock on the estuarine side of Sapelo Island were investigated over a period of 11 months using a combination of groundwater and surface water samples. The primary source of chloride and sulfate in the aquifer is the saline waters in the bordering river and marsh. Physical and chemical parameters varied little during this 11-month study, suggesting that lateral advection away from the center of the freshwater lens toward both the river and the salt marsh balances chemical diffusion of ions from the saline portions of the groundwater towards the aquifer's interior. This advective transport must be in an approximate steady-state to produce such a stable distribution of chemical species within the groundwater over the course of this study.

Chemical gradients in Fe^{2+}, Mn^{2+}, $\sum H_2S$, and DOC occur at the salinity transitions on both sides of the freshwater lens. These gradients did not vary significantly over time, except in the wells with the highest concentrations of Fe^{2+} and $\sum H_2S$. These findings seem to indicate that microbial iron reduction and, to a lesser extent, sulfate reduction occur simultaneously and generate enough reductants (i.e. Fe^{2+} and $\sum H_2S$) that then diffuse laterally to reduce manganese oxides chemically. Our results also suggest that metal reducing bacteria can outcompete sulfate reducing bacteria in the subsurface even at high sulfate concentrations if oxygen is episodically introduced by recharge in the middle of the hammock to keep the groundwater in suboxic conditions and maintain a dynamic cycle between Fe^{2+} and iron oxides.

It has been shown that the generation of CO_2 during aerobic and anaerobic respirations of natural organic matter may increase the dissolution of carbonate minerals (Valocchi et al., 1981; Appelo et al., 1990; Moore, 1999), with important environmental consequences (Paull et al., 1990). In this system, the low activity of sulfate reducing bacteria may prevent accumulation of large concentrations of dissolved inorganic carbon and limit the extent of carbonate mineral dissolution.

Acknowledgements

This study was supported by grants to C.R. from the USGS Water Resources Institute program for the State of Georgia, administered by A. Georgakakos, and from the NSF Long Term Ecological Research program for Georgia Coastal Ecosystems OCE 9982133. These grants and the School of Earth and Atmospheric Sciences at Georgia Tech provided salary support for M.S. We thank M. Schreiber for her advice on MLS design and installation, S. Sibley for providing DOC data, G. Schultz for use of unpublished geophysical data and analyses of groundwater flow at the site, K. Hunter for assistance with sampling and analyses, and numerous undergraduate

classes and researchers for their contributions to field and laboratory work. S. Bottrell and W. Moore provided comments that improved the manuscript.

References

Appelo, C.A.J., Willemsen, A., 1987. Geochemical calculations and observations on salt water intrusions, I. A combined geochemical/mixing cell model. Journal of Hydrology 97, 313–330.

Appelo, C.A.J., Willemsen, A., Beekman, H.E., Griffioen, J., 1990. Geochemical calculations and observations on salt water intrusions 2. Validation of a geochemical model with column experiments. Journal of Hydrology 120, 225–250.

Arakaki, T., Morse, J.W., 1993. Coprecipitation and adsorption of Mn(II) with mackinawite (FeS) under conditions similar to those found in anoxic sediments. Geochimica et Cosmochimica Acta 57, 9–14.

Barker, A.P., Newton, R.J., Bottrell, S.H., 1998. Processes affecting groundwater chemistry in a zone of saline intrusion into an urban sandstone aquifer. Applied Geochemistry 13(6), 735–749.

Bottrell, S.H., Smart, P.L., Whitaker, F., Raiswell, R., 1991. Geochemistry and isotope systematics of sulphur in the mixing zone of Bahamian blue holes. Applied Geochemistry 6, 97–103.

Bourg, A.C.M., Bertin, C., 1994. Seasonal and spatial trends in manganese solubility in alluvial aquifer. Environmental Science and Technology 28(5), 868–876.

Brown, C.J., Coates, J.D., Schoonen, M.A.A., 1999. Localized sulfate-reducing zones in a coastal plain aquifer. Ground Water 37(4), 505–516.

Burdige, D.J., Nealson, K.H., 1985. Chemical and microbiological studies of sulfide-mediated manganese reduction. Geomicrobiology Journal 4(4), 361–387.

Cai, W.-J., Wang, Y., Krest, J., Moore, W.S., 2003. The geochemistry of dissolved inorganic carbon in a surficial groundwater aquifer in North Inlet, South Carolina, and the carbon fluxes to the coastal ocean. Geochimica et Cosmochimica Acta 67(4), 631–637.

Champ, D.C., Gulens, J., Jackson, R.E., 1979. Oxidation–reduction sequences in ground-water systems. Canadian Journal of Earth Sciences 16, 1466–1472.

Chapelle, F.H., 1997. The Hidden Sea, Geoscience Press, Tucson, AZ, 238 pp.

Chapelle, F.H., Lovley, D.R., 1992. Competitive exclusion of sulfate reduction by Fe(III)-reducing bacteria: a mechanism for producing discrete zones of high-iron ground water. Ground Water 30(1), 29–36.

Charette, M.A., Sholkovitz, E.R., 2002. Oxidative precipitation of groundwater-derived ferrous iron in the subterranean estuary of a coastal bay. Geophysical Research Letters 29(10), 85(1-4).

Charette, M.A., Buesseler, K.O., Andrews, J.E., 2001. Utility of radium isotopes for evaluating the input and transport of groundwater-derived nitrogen to a Cape Cod estuary. Limnology and Oceanography 46(2), 465–470.

Cline, J.D., 1969. Spectrophotometric determination of hydrogen sulfide in natural waters. Limnology and Oceanography 14, 454–458.

Dickson, A.G., 1993. pH buffers for seawater media based on the total hydrogen ion concentration scale. Deep-Sea Research 42, 107–118.

Gran, G., 1952. Determination of the equivalence point in potentiometric titration. Part II. Analyst 77, 661–671.

Groffman, A.R., Crossey, L.J., 1999. Transient redox regimes in a shallow aquifer. Chemical Geology 161, 415–442.

Jakobsen, R., Postma, D., 1999. Redox zoning, rates of sulfate reduction and interactions with Fe-reduction and methanogenesis in a shallow sandy aquifer, Romo, Denmark. Geochimica et Cosmochimica Acta 63(1), 137–151.

Magaritz, M., Luzier, J.E., 1985. Water rock interactions and seawater–freshwater mixing effects in the central dunes aquifer, Coos Bay, Oregon. Geochimica et Cosmochimica Acta 49, 2515–2525.

Matsunaga, T., Karametaxas, G., Von Gunten, U.H., Lichtner, P.C., 1993. Redox chemistry of iron and manganese minerals in river-recharged aquifers: a model interpretation of a column experiment. Geochimica et Cosmochimica Acta 57, 1691–1704.

Moore, W.S., 1996. Large groundwater inputs to coastal waters revealed by ^{226}Ra enrichments. Nature 380, 612–614.

Moore, W.S., 1999. The subterranean estuary: a reaction zone of ground water and sea water. Marine Chemistry 65, 111–125.

Myers, C.R., Nealson, K.H., 1988. Microbial reduction of Mn oxides: interactions with iron and sulfur. Geochimica et Cosmochimica Acta 52, 2727–2732.

Nyffeler, U.P., Li, Y.-H., Santschi, P.H., 1984. A kinetic approach to describe trace-element distribution between particles and solution in natural aquatic systems. Geochimica et Cosmochimica Acta 48, 1513–1522.

Parkhurst, D.L., 1995. User's guide to PHREEQC—a computer program for speciation, reaction-path, advective-transport, and inverse geochemical calculations. US Geological Survey Water-Resources Investigations Report 95-4227, 143 p.

Paull, C.K., Speiss, F., Curry, J., Twichell, D., 1990. Origin of Florida canyon and the role of spring snapping on the formation of submarine box canyons. Geological Society of America Bulletin 102, 502–515.

Portnoy, J.W., Nowicki, B.L., Roman, C.T., Urish, D.W., 1998. The discharge of nitrate-contaminated groundwater from developed shoreline to marsh-fringed estuary. Water Resources Research 34(11), 3095–3104.

Postma, D., 1985. Concentration of Mn and separation from Fe in sediments—I. Kinetics and stoichiometry of the reaction between birnessite and dissolved Fe(II) at 10 °C. Geochimica et Cosmochimica Acta 49, 1023–1033.

Pyzik, A.J., Sommer, S.E., 1981. Sedimentary ion monosulfides: kinetics and mechanism of formation. Geochimica et Cosmochimica Acta 45, 687–698.

Schultz, G., 2002. Hydrologic and geophysical characterization of spatial and temporal variations in coastal aquifer systems. PhD thesis, Georgia Institute of Technology, 355 pp.

Schultz, G., Ruppel, C., 2000. Geophysical and hydrologic characterization of spatial and temporal variations in

the distribution of freshwater and saltwater at the island–estuary interface. Sapelo Island National Estuarine Research Reserve, NOAA-NERRS Final Report, 113 pp.

Schultz, G., Ruppel, C., 2002. Constraints on hydraulic parameters and implications for groundwater flux across the upland–estuary interface. Journal of Hydrology 260, 255–269.

Skoog, D.A., Leary, J.L., 1996. Principles of instrumental analysis, Saunders College Publishing.

Snyder, M., 2002. Geochemical trends associated with the seawater–freshwater mixing zone in a surficial coastal aquifer. Sapelo Island, GA. MS Thesis, Georgia Institute of Technology, 148 pp.

Stites, W., Chambers, L.W., 1991. A method for installing miniature multilevel sampling wells. Ground Water 29, 430–432.

Stookey, L.L., 1970. Ferrozine: a new spectrophotometric reagent for iron. Analytical Chemistry 42, 779–781.

Testa, J.M., Charette, M.A., Sholkovitz, E.R., Allen, M.C., Rago, A., Herbold, C.W., 2002. Dissolved iron cycling in the subterranean estuary of coastal bays: Waquoit Bay, Massachussetts. Biological Bulletin 203, 255–256.

Tobias, C.R., Macko, S.A., Anderson, I.C., Canuel, E.A., Harvey, J.W., 2001a. Tracking the fate of a high concentration groundwater nitrate plume through a fringing marsh: a combined groundwater tracer and in situ isotope enrichment study. Limnology and Oceanography 46(8), 1977–1989.

Tobias, C.R., Harvey, J.W., Anderson, I.C., 2001b. Quantifying groundwater discharge through fringing wetlands to estuaries: seasonal variability, methods comparison, and implications for wetland–estuary exchange. Limnology and Oceanography 46(3), 604–615.

Urish, D.W., 1980. Asymmetric variation of Ghyben-Herzberg lens. Journal of Hydraulics Division, Proceedings of the American Society of Civil Engineers 107, 1149–1158.

Valelia, I., Costa, J., Teal, J.M., Howes, B., Aubrey, D., 1990. Transport of groundwater-borne nutrients from watersheds and their effects on coastal waters. Biogeochemistry 10, 177–197.

Valelia, I., Foreman, K., LaMontagne, M., Hersch, D., Costa, J., Pechol, P., DeMeo Anderson, B., D'Avanzo, C., Babione, M., Sham, C.-H., Brawley, J., Lajtha, K., 1992. Coupling of watersheds and coastal waters: sources and consequences of nutrient enrichment in Waquoit Bay, Massachussetts. Estuaries 15, 443–457.

Valocchi, A.J., Street, R.L., Roberts, P.V., 1981. Transport of ion-exchanging solutes in groundwater: chromatographic theory and field simulation. Water Resources Research 17(5), 1517–1527.

Von Gunten, U., Zobrist, J., 1993. Biogeochemical changes in groundwater-infiltration systems: column studies. Geochimica et Cosmochimica Acta 57, 3895–3906.

Von Gunten, U.H., Karametaxas, G., Krahenbuhl, U., Kuslys, M., Giovanoli, R., Hoehn, E., Keil, R., 1991. Seasonal biogeochemical cycles in riverborne groundwater. Geochimica et Cosmochimica Acta 55, 3597–3609.

Yao, W., Millero, F.J., 1996. Oxidation of hydrogen sulfide by hydrous Fe(III) oxides in seawater. Marine Chemistry 52, 1–16.